THE UNIVERSITY OF MICHIGAN

COLLEGE OF ENGINEERING
Department of Engineering Mechanics
Department of Mechanical Engineering

Tire and Suspension Systems Research Group

Technical Report No. 6

THE PLANE ELASTIC CHARACTERISTICS OF CORD-RUBBER LAMINATES-II

R. N. Dodge
N. L. Field
S. K. Clark

Project Directors: S. K. Clark and R. A. Dodge

ORA Project 02957

administered through:

OFFICE OF RESEARCH ADMINISTRATION ANN ARBOR

June 1961

en gn

UMR0652

The Tire and Suspension Systems Research Group
at The University of Michigan is sponsored by:

FIRESTONE TIRE AND RUBBER COMPANY

GENERAL TIRE AND RUBBER COMPANY

B. F. GOODRICH TIRE COMPANY

GOODYEAR TIRE AND RUBBER COMPANY

UNITED STATES RUBBER COMPANY

TABLE OF CONTENTS

		Page
LIST OF FIGURES		vii
NOMENCLATURE		ix
I.	FOREWARD	1
II.	SUMMARY	3
III.	COMPARISON BETWEEN EXPERIMENT AND THEORY FOR CORD-RUBBER LAMINATES OF TYPE 1	5
IV.	COMPARISON BETWEEN EXPERIMENT AND THEORY FOR CORD-RUBBER LAMINATES OF TYPE 2	19
APPENDIX:	SAMPLE CALCULATIONS FOR CORRECTION OF CORD ANGLE DUE TO STRAIN	33
V.	ACKNOWLEDGMENT	35
VI.	REFERENCE	37
VII.	DISTRIBUTION LIST	39

LIST OF FIGURES

Figure		Page
1.	Modulus E_ξ vs. cord half angle α, as predicted from Eq. (15) of Ref. 1, along with corrected experimental values of E_ξ, for a Type 1 structure.	8
2.	Cross-modulus $F_{\xi\eta}$ vs. cord half angle α, as predicted from Eq. (15) of Ref. 1, along with corrected experimental values of $F_{\xi\eta}$, for a Type 1 structure.	9
3.	Mohr's strain circle for equal principal strains.	10
4.	Equipment for applying axial loads, torque, and internal pressure simultaneously, along with measuring apparatus.	13
5.	Recording equipment used in the tests illustrated in Fig. 4.	14
6.	Detailed view of measuring device used to obtain angle of twist in the tests shown in Fig. 4.	15
7.	Shear modulus $G_{\xi\eta}$ vs. cord half angle α, as predicted from Eq. (17) of Ref. 1, along with experimental values of $G_{\xi\eta}$, for a Type 1 structure.	18
8.	General plane state of stress on each ply of a two ply structure.	21
9.	Ratio σ_ξ/ϵ_ξ vs. cord half angle α, as predicted from Eq. (5) of this report with $\sigma_\eta = \sigma_{\xi\eta} = 0$, along with experimental values of this ratio, for a Type 2 structure.	26
10.	Ratio σ_ξ/ϵ_η vs. cord half angle α, as predicted from Eq. (5) of this report with $\sigma_\eta = \sigma_{\xi\eta} = 0$, along with experimental values of this ratio, for a Type 2 structure.	27
11.	Ratio $\sigma_{\xi\eta}/\epsilon_{\xi\eta}$ vs. cord half angle α, as predicted from Eq. (5) of this report with $\sigma_\eta = \sigma_\xi = 0$, along with experimental values for this ratio, for a Type 2 structure.	28

NOMENCLATURE

English Letters:

a_{ij}	Constants associated with generalized Hooke's law, using properties based on cord tension.
a'_{ij}	Constants associated with generalized Hooke's law, using properties based on cord compression.
E,F,G	Elastic constants for orthotropic laminates with cords in tension.
E',F',G'	Elastic constants for orthotropic laminates with cords in compression.

Greek Letters:

α	One-half the included angle between cords in adjoining plies in a two-ply laminate.
ϵ	Strain
μ	Poisson's ratio
ξ,η	Orthogonal co-ordinates aligned along and normal to the principal axes of elasticity, or orthotropic axes, in an orthotropic laminate. These directions are the bisectors of the cord angles.
σ	Stress
σ'	Interply stress
σ^*	External stress acting on a ply whose cords are in tension.
σ^{**}	External stress acting on a ply whose cords are in compression.
σ^+	Combined external and interply stress acting on a ply whose cords are in tension.
σ^{++}	Combined external and interply stress acting on a ply whose cords are in compression.

I. FOREWARD

In October 1960, a series of technical reports was issued by the Tire and Suspension Systems research group at The University of Michigan. Among these reports was Ref. 1, which dealt with the plane elastic characteristics of cord-rubber laminates. In that report, the basic theoretical approach used in determining these elastic characteristics was laid out and was accompanied by the experimental results available at that time. Since then, more experimental evidence has become available concerning the elastic characteristics of such laminates and a greater insight has been obtained into the meaning of some of the equations which may be used to calculate these characteristics. In particular, a much better understanding now exists of the equations which describe the elastic action of a cord-rubber laminate when some of the cords are in compression and some are in tension. Experimental evidence concerning this type of structure is also now available. For these reasons it was felt that this new information should be collected and issued.

A very natural division arises between two common types of cord-rubber laminates. In one type, called throughout the body of this report "Type 1," the structure is orthotropic in the sense that shear and normal effects are not coupled. This type of structure normally arises when alternate plies are laid up at equal angles to some common midline and when all the cords of the structure are either in tension or in compression. This type of

structure could also arise due to any symmetrical order of lamination in which either pure cord tension or pure cord compression prevailed, or finally could arise in rare cases from certain unique combinations of cord materials and cord angles. The basic requirement for all Type 1 structures is that they do not exhibit elastic coupling between normal and shearing effects. Any structure satisfying this requirement is given the name "orthotropic." All other non-isotropic structures may be lumped into the general classification of anisotropic. The most common form of anisotropy, from the point of view of the manufacturer of pneumatic tires, is the usual symmetrical tire carcass structure in which some cords are in a state of compression while others are in a state of tension. Our experimental studies have led us to believe that these structures, called throughout the body of this report "Type 2," are considerably more prevalent than we had originally thought. It is therefore probable that in the study of a real pneumatic tire their characteristics will be of some importance.

II. SUMMARY

This supplementary report contains additional experimental and analytical results concerning the determination of plane elastic characteristics of cord-rubber laminates. These results are an extension of those presented in Ref. 1, with the emphasis placed somewhat on those types of structures composed of an even number of plies in which the cord strain is of opposite sign in adjoining plies, i.e., Type 2 structures. The basic theoretical approach of Ref. 1 has not been altered, but its use has been extended to include this type of structure.

In the development presented in Ref. 1 a statically indeterminate set of equations arises which can only be solved with the aid of some simplifying assumptions. In this present supplement it has been shown that these equations can be solved exactly if one does not attempt to separate the interply stress from the applied stress. A digital computer program has been written which solves these equations and yields the plane elastic characteristics. Some results from this program are presented in this report.

With the addition of this report a more complete analysis of plane elastic characteristics of cord-rubber laminates is at hand. It is now possible to calculate the elastic properties of all basic types of cord-rubber laminates knowing only the elastic properties of a single sheet of its constituent material.

III. COMPARISON BETWEEN EXPERIMENT AND THEORY FOR CORD-RUBBER LAMINATES OF TYPE 1

Cord-rubber laminates of Type 1, as previously defined, are most easily obtained by constructing an even number of plies with equal alternating cord angles and then applying loads in such a way that the stiffnesses of cords in each laminate are the same. For textile cords, this is most easily obtained by causing all cords to go into tension or into compression. Provided that the thickness of such a sheet of plies is small compared to the dimensions of the structures made from this sheet, then this material has been shown to follow closely equations developed for a plane orthotropic material. Equations (15) and (17) of Ref. 1 give the basic elastic characteristics of such a structure in terms of the elastic constants of a single sheet of this structure. These equations are repeated for convenience.

$$\boxed{\begin{gathered}\frac{1}{E_\xi} = \left(a_{11} - \frac{a_{13}^2}{a_{33}}\right) \qquad \frac{1}{E_\eta} = \left(a_{22} - \frac{a_{23}^2}{a_{33}}\right) \\ \frac{1}{F_{\xi\eta}} = \left(a_{12} - \frac{a_{13}a_{23}}{a_{33}}\right)\end{gathered}} \tag{1}$$

$$\boxed{\begin{gathered}\frac{1}{G_{\xi\eta}} = \left\{ - a_{31}\left[\left(\frac{a_{12}}{a_{11}}\right)\frac{(a_{12}a_{13}-a_{11}a_{23})}{(a_{11}a_{22}-a_{12}^2)} + \frac{a_{13}}{a_{11}}\right] \right. \\ \left. + (a_{32})\frac{(a_{12}a_{13}-a_{11}a_{23})}{(a_{11}a_{22}-a_{12}^2)} + a_{33}\right\}\end{gathered}} \tag{2}$$

Reference 1 presents a complete analysis of Type 1 laminates as previously defined. In addition, certain experimental data available at that time were compared to predictions concerning elastic stiffnesses made on the basis of this theory. Agreement between measured and predicted elastic stiffnesses was shown to be quite good. At that time no method had been found for experimentally producing shear in a Type 1 structure, since the application of shearing stresses tends to put some cords in tension and some in compression in the usual type of laminate. Therefore, the information presented in Ref. 1 was not complete since the shear modulus of orthotropic laminates was not verified by experimental measurement. Subsequent to that report, a method was devised which has allowed the measurement of the shear modulus of Type 1 laminates, and has resulted in experimental values close to that predicted by Eq. (2). This experiment was set up and run and its results will be reported here along with some corrections to the experimentally determined data reported in Ref. 1 on extensional stiffnesses.

During the extension or compression of the tubular specimens used here, angular changes take place between cords in adjacent plies. In view of the fact that the stiffnesses measured in these experiments are taken not at zero load but rather at a strain of approximately 3% in the specimen, a correction factor may be applied to the data obtained in order to account for the change in angle associated with a 3% strain. In some cases this angular change is small while in other cases it is significant. In either event, the specimen should actually be considered at its instantaneous cord angle,

not at the original cord angle at which it was constructed. For that reason some of the curves of Ref. 1 pertaining to the agreement between calculated and experimental stiffness and cross moduli are reproduced in Figs. 1 and 2 with the appropriate angular corrections indicated on the curves. It is seen that as a rule these corrections cause the experimental data to fall even closer to the calculated stiffness than previously; and that, if strains can remain in this approximate region, or order of magnitude, in a real pneumatic tire, then it is probably not necessary to correct elastic stiffnesses for changing angle in tire calculations since the differences are not usually large.

Attention is next directed to the considerably harder problem of experimentally measuring the shear modulus of Type 1 laminate, such as predicted by Eq. (2) of this report. The fundamental difficulty involved here is to find some way of insuring that all cords in the circular tube remain in a state of tension sufficiently great so that their tensile modulus is developed. It is difficult to obtain this because, as mentioned previously, the application of shear stresses tends to cause one set of cords to go into compression while the other set goes into tension. One solution to this problem is to preload the cords thoroughly before applying torque.

Due to the low stiffness of these cylindrical specimens in certain directions, it is not possible to load the cords properly by applying large axial force and internal pressure at random, since to do so might cause excessive deformation of the structure, with possible damage to interply bonds. It is necessary to apply the loads carefully in a manner determined by analysis.

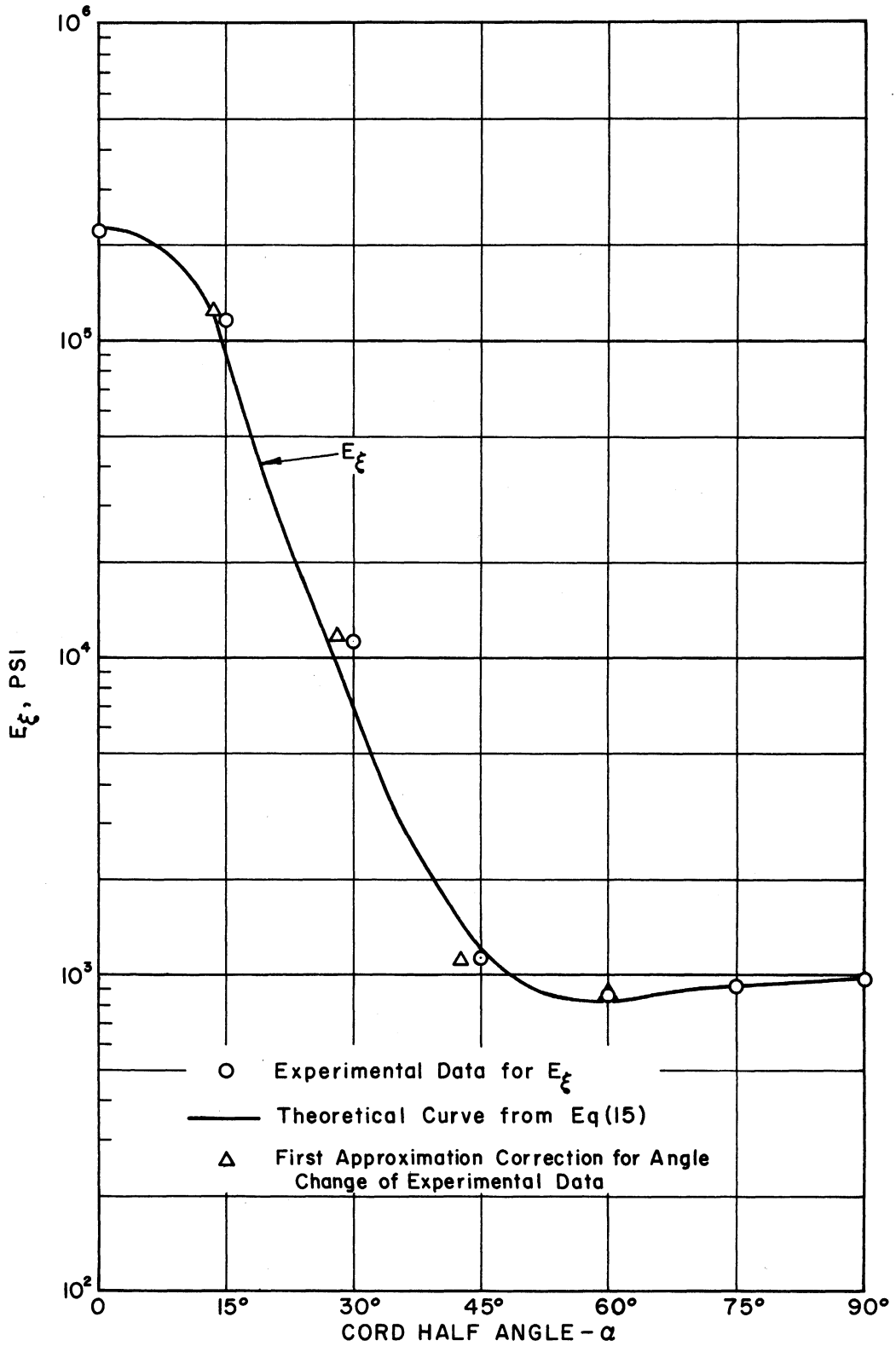

Fig. 1. Modulus E_ξ vs. cord half angle α, as predicted from Eq. (15) of Ref. 1, along with corrected experimental values of E_ξ, for a Type 1 structure.

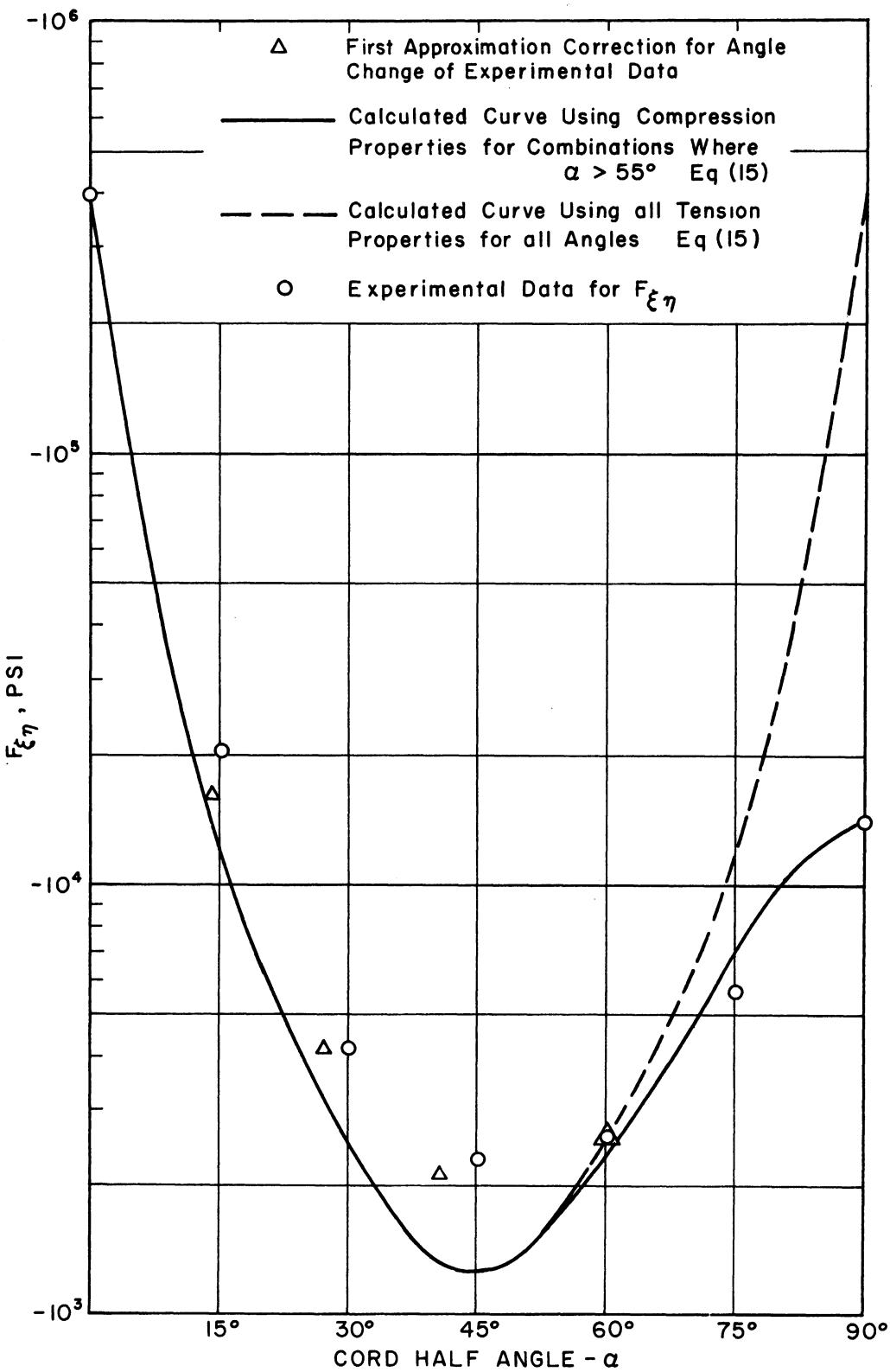

Fig. 2. Cross-modulus $F_{\xi\eta}$ vs. cord half angle α, as predicted from Eq. (15) of Ref. 1, along with corrected experimental values of $F_{\xi\eta}$, for a Type 1 structure.

The basic stress-strain relations for orthotropic structures are used for this analysis. These were originally given as Eqs. (5) of Ref. 1 but are repeated here in the form applicable to this case

$$\epsilon_\xi = \frac{\sigma_\xi}{E_\xi} - \frac{\sigma_\eta}{F_{\xi\eta}}$$

$$\epsilon_\eta = \frac{\sigma_\eta}{E_\eta} - \frac{\sigma_\xi}{F_{\xi\eta}} \tag{3}$$

where the ξ direction may now be taken along the longitudinal axis of the tube while the η direction is tangential to the tube. It may be seen from Fig. 3 that if $\epsilon_\xi = \epsilon_\eta$, then the corresponding Mohr's strain circle is a point. This is valid for an orthotropic material since it is a result of pure geometry and is independent of Eqs. (3). Further, if the strain conditions are such as shown in Fig. 3, then the strain in any direction on the tube, and specifically in the cord directions, is also equal to ϵ_ξ or ϵ_η.

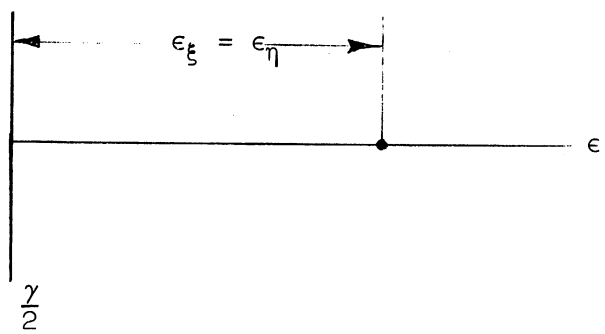

Fig. 3. Mohr's strain circle for equal principal strains.

It is believed that this is a very convenient design criterion for the preloading of cords.

Setting $\epsilon_\xi = \epsilon_\eta$, the stresses and associated loads on the cylinders in question here may be determined. These are given in Table I for various values of the cord strains. Note that in general axial loads and internal pressure must be used simultaneously to achieve the desired cord strain. In the experiments reported here, cord strains ranging from .003 to .005 were chosen as values for the preloading of cords.

The method used here for obtaining these compound loads was to convert a standard torsion testing machine into a combined tension-torsion-internal pressure testing device. This was accomplished by designing special fixtures which allowed the insertion of a hydraulic cylinder between the working heads of a standard torsion testing machine. In this way, an axial load or an internal pressure could be applied to a cylindrical specimen prior to twisting it. It was necessary, of course, to take precautions to insure that the torsional moments did not influence the axial forces and vice versa. For structural reasons it was also necessary to construct a load-carrying frame around the cylindrical specimen so that the tensile loads imposed by the hydraulic cylinder were carried by the frame rather than by the torsion machine, since this machine was not designed to transmit tensile loads through its working heads. This apparatus is illustrated in the photographs of Figs. 4, 5, and 6. In addition to the mechanism for applying loads, it was also necessary to measure internal pressure, axial load, torque, and angle of twist simultaneously. By avoiding coupling between tensile and torsional loads, it was possible to preset the axial load to a given value by use of a hydraulic cylinder, hand-operated piston pump,

TABLE I

Test Specimen	σ_ξ psi	σ_η psi	Radius r in.	Thickness t in.	Area A in.^{2}	Load Combination		ϵ_ξ in./in.	ϵ_η in./in.
						Axial Load Lbs.	Internal Pressure psi		
30° - No. 1	506	171	3.140	.205	3.912	1642	11.2	.003	.003
30° - No. 2	506	171	3.145	.205	3.919	1646	11.2	.003	.003
45° - No. 1	542	542	3.185	.204	3.952	1078	34.8	.005	.005
45° - No. 2	542	542	3.180	.203	3.927	1070	34.6	.005	.005
60° - No. 1	285	842	3.205	.212	4.128	-558	55.7	.005	.005
60° - No. 2	285	842	3.190	.202	3.921	-530	53.4	.005	.005

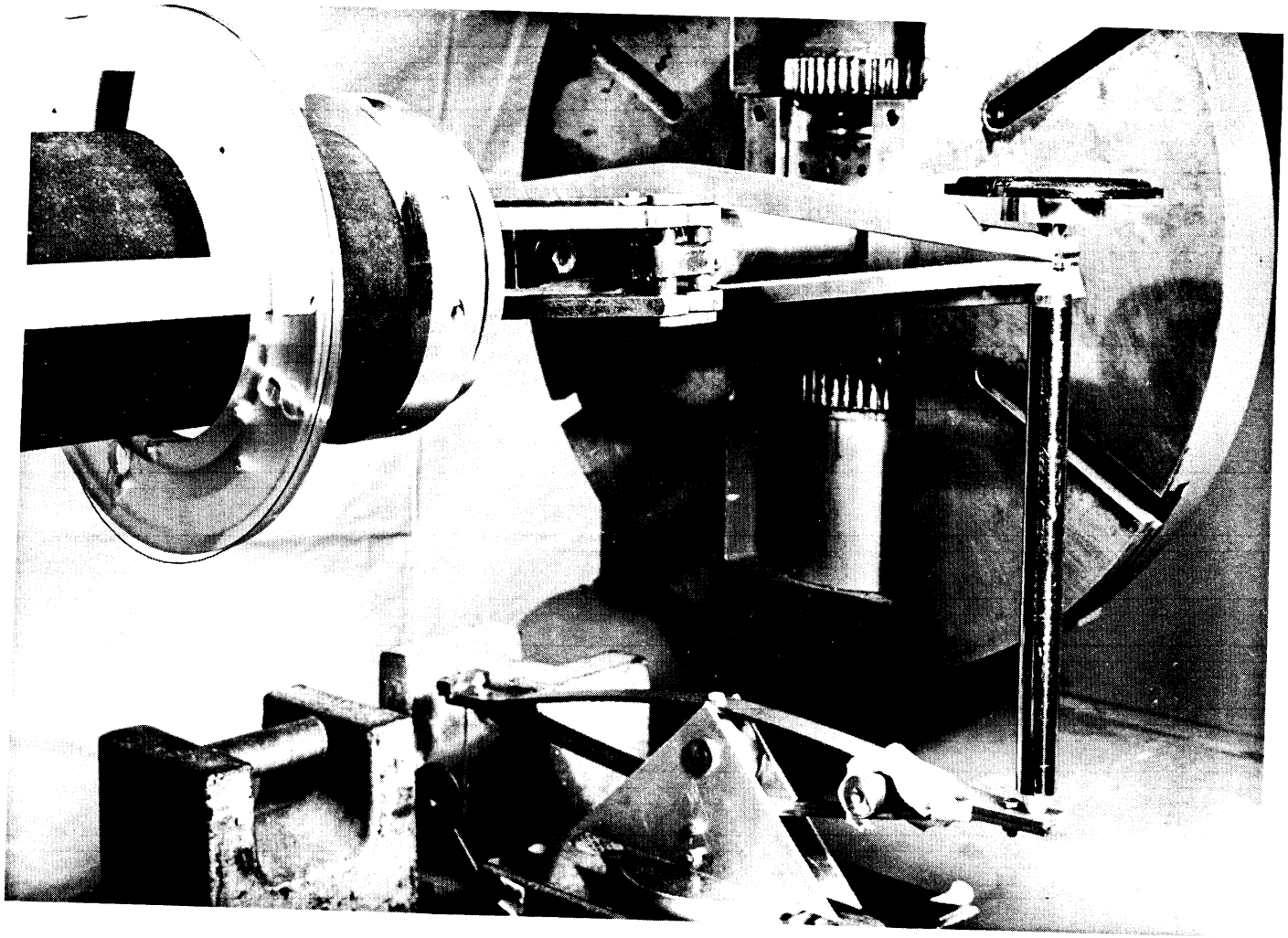

Fig. 4. Equipment for applying axial loads, torque, and internal pressure simultaneously, along with measuring apparatus.

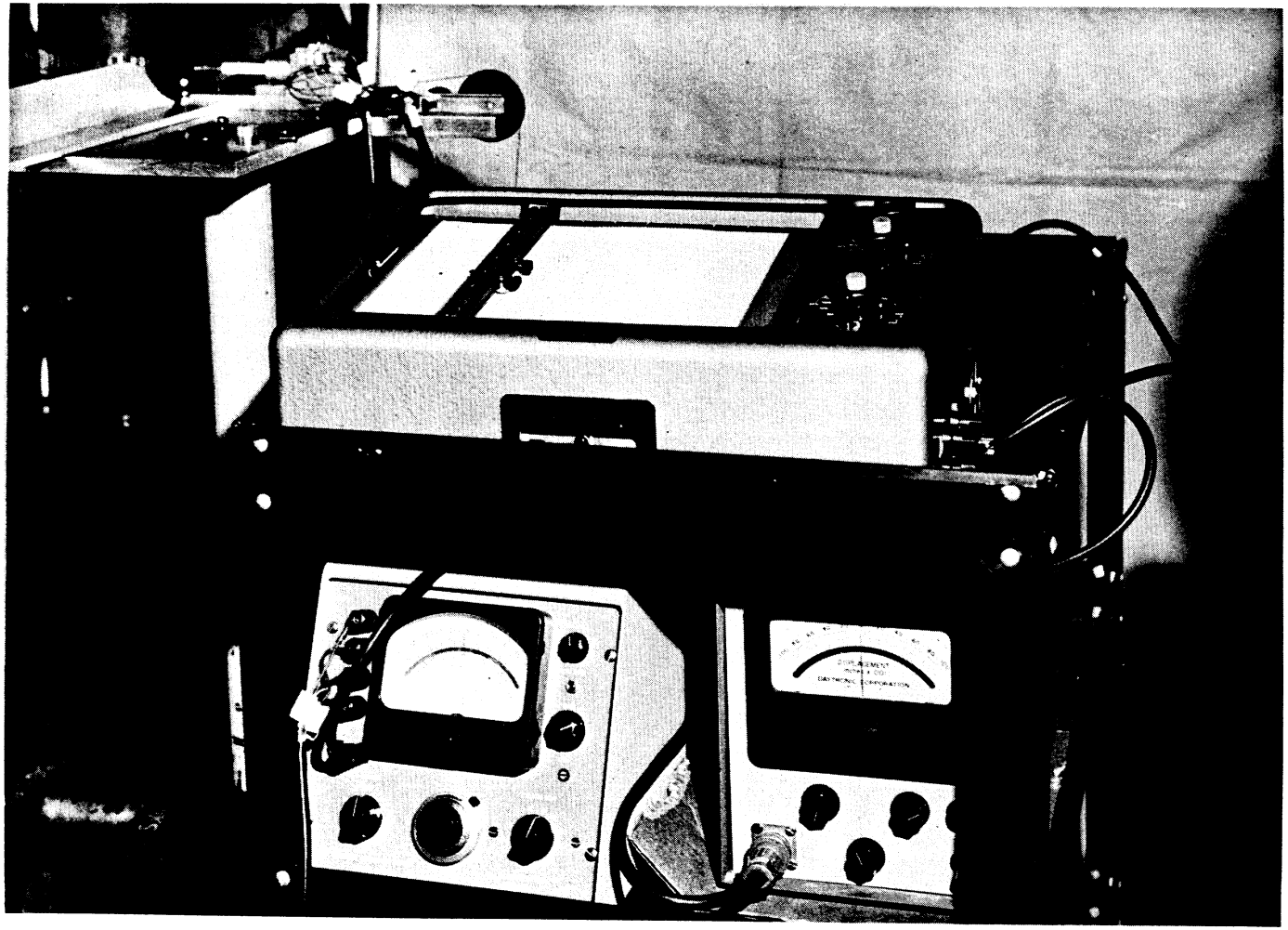

Fig. 5. Recording equipment used in the tests illustrated in Fig. 4.

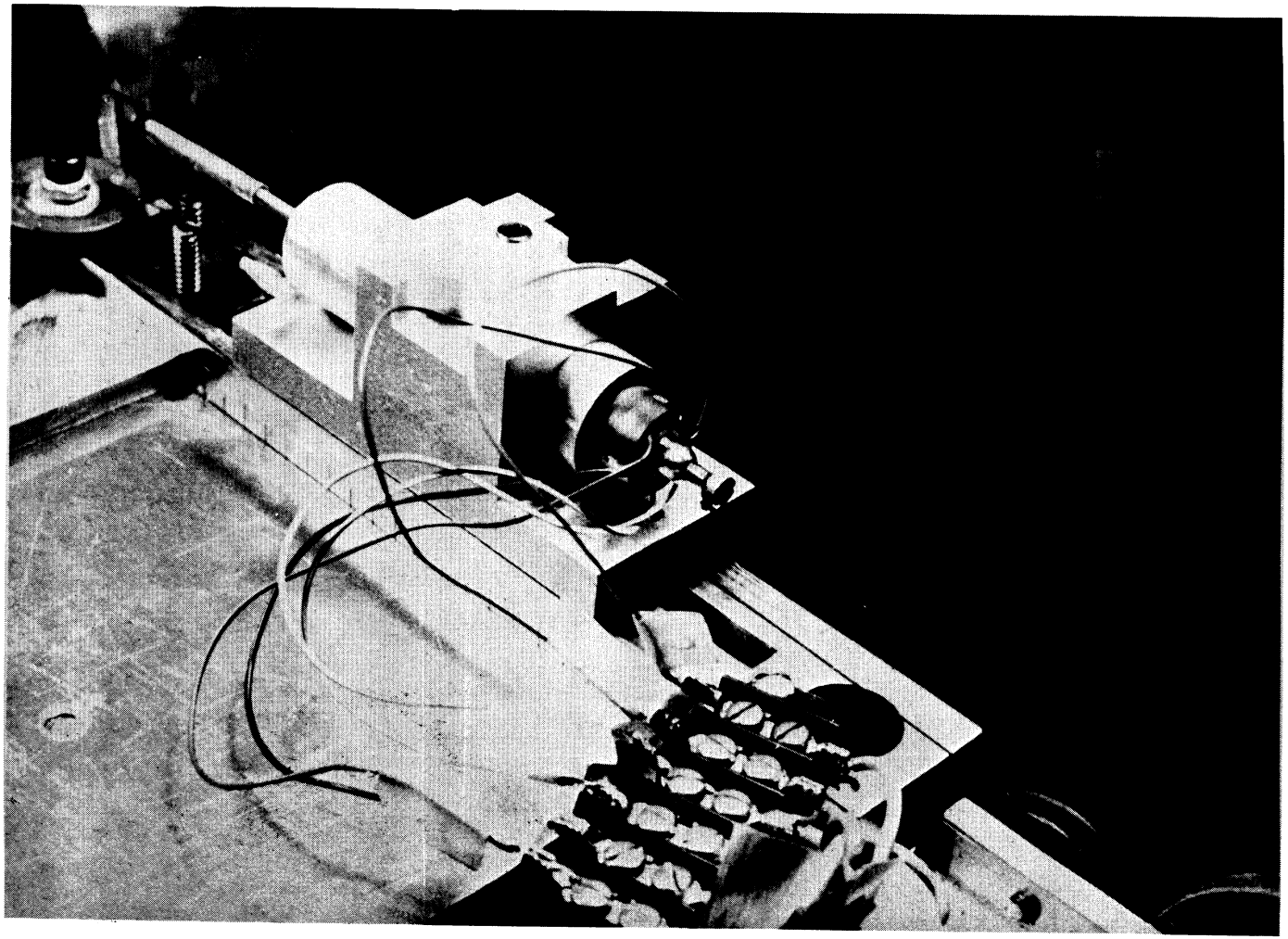

Fig. 6. Detailed view of measuring device used to obtain angle of twist in the tests shown in Fig. 4.

and gauge system. Internal pressure was set by a gauge and nitrogen bottle arrangement. These pressures could be held constant by closing the system tightly, with only periodic checks and adjustments. The moving head of the torsion machine was then rotated to cause twist of the specimen.

Measurement of applied torque utilized a lever arm which connected to a standard Baldwin load cell. Angle of twist in the specimen was measured by use of a relative motion troptometer manufactured from an ordinary Schaevitz linear differential transformer. The windings of this transformer were attached to a small cart running in a ball bearing track. The core of the transformer was suspended independently by a string mechanism and the cart and core were each attached by means of nylon cord running over pulleys to different circular disks mounted some distance apart on the specimen. The differences in angle of rotation of the two disks caused a difference in the relative motion of the windings and the core of the transformer so that this difference in relative motion resulted in an output voltage of the transformer when the cores were excited by an AC excitation.

Measurements of applied torque and angle of twist were made simultaneously by feeding the output voltage from the Baldwin load cell into the y-axis of a Moseley x-y recorder, while the output voltage from the differential transformer was fed to the x-axis of the recorder. This allowed a simultaneous record of torque versus angle of twist to be made in such a way that by a simple scale change the shear modulus of each specimen could be determined.

The results of these experiments are compared in Fig. 7 with the calculations made on the basis of a shear modulus being defined for a structure which had all of its cords in a state of tension. It may be seen that the agreement between the experimental data and the calculations is quite acceptable. It should also be noted that in Fig. 7 the calculated value of shear modulus, assuming all cords to be in a state of compression, is also presented for comparison. This condition results in shear stiffnesses considerably lower than that obtained when all cords are in a state of tension.

A set of problems similar to those encountered in shear modulus measurements did not arise during our original work on the measurement of elastic extensional stiffnesses. The reason for this was that the nature of the cord rubber laminates is such that cord tensions may be easily obtained by axial loads at those angles where the cords are important to the over-all stiffness of the structure, while in those regions where it is difficult to induce cord tension, the nature of the structure is such that the rubber surrounding the cords primarily determines the stiffness of the specimen.

It was not possible to attempt a correlation with experiment of Eq. (2), using compression properties of the sheet, since the thin-walled nature of the cylindrical tubes prevented compressive axial loads from being applied to the specimen. At this time no simple way is known to force all cords into compression other than this. For that reason, no further work will be done at the present on measurement of the shear modulus of Type 1 structures under conditions of cords being in compression.

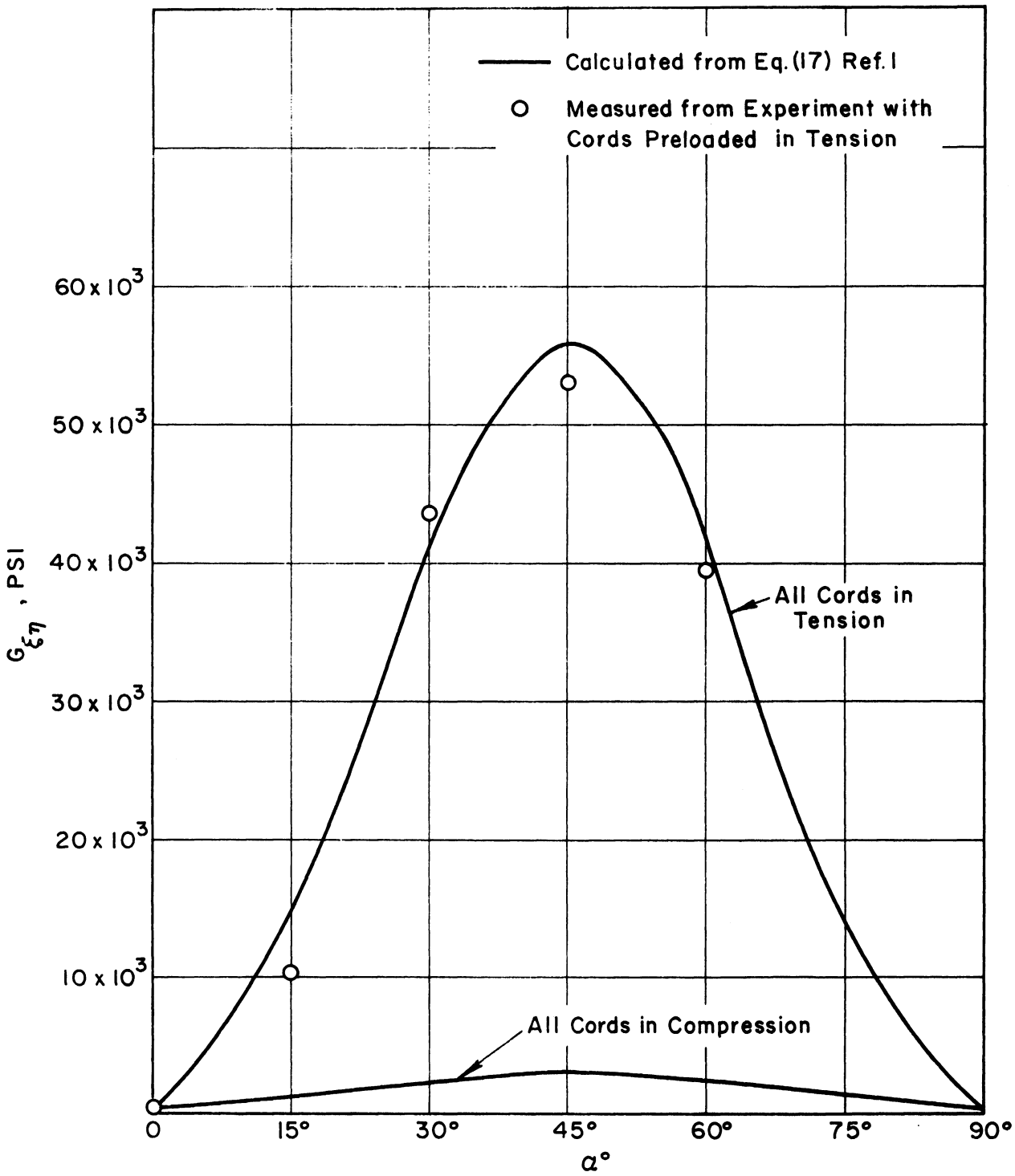

Fig. 7. Shear modulus $G_{\xi\eta}$ vs. cord half angle α, as predicted from Eq. (17) of Ref. 1, along with experimental values of $G_{\xi\eta}$, for a Type 1 structure.

IV. COMPARISON BETWEEN EXPERIMENT AND THEORY FOR CORD-RUBBER LAMINATES OF TYPE 2

Cord-rubber laminates of Type 2 have been previously defined as those which are generally anisotropic in their nature and not specifically orthotropic. The terminology, "Type 2 laminates," is adopted for convenience and conciseness since most of the instances in which this type of structure arises are caused by a symmetrical laminated structure being loaded in such a way that some of the textile cords move into a state of tension while others move into a state of compression. This causes different stiffnesses in the different plies with the resulting loss of orthotropy. The structure then becomes generally anisotropic, both in respect to plane and bending properties, with the consequence that simple orthotropic elastic constants cease to exist for such a structure. One must fall back on the general statement of Hooke's Law for such a plane structure and must use the ratios of the various strains to the various stresses as measures of elastic stiffness. This is not a very satisfactory situation from the physical point of view since the coupling between shear and normal stresses confuses the physical interpretation which one would like to place upon the various ratios of stresses to strains. For these reasons the whole subject of Type 2, or anisotropic, laminates is considerably harder to visualize as well as being somewhat more cumbersome to deal with analytically, than are orthotropic laminates.

Reference 1 outlined the equations which must be used for the study

of these laminates. These were based on an assumed two-ply structure such as shown in Fig. 8. Writing one set of equations for each of the two plies, assuming one ply to be in a state of cord tension while the other ply is in a state of cord compression, one obtains a set of equations describing the composite structure which were originally given as Eqs. (22) of Ref. 1. These equations are repeated here as Eqs. (4).

Ply 1

$$\epsilon_\xi = [a_{11}(+\alpha)](\sigma_\xi^* + \sigma_\xi') + [a_{12}(+\alpha)](\sigma_\eta^* + \sigma_\eta') + [a_{13}(+\alpha)](\sigma_{\xi\eta}^* + \sigma_{\xi\eta}')$$

$$\epsilon_\eta = [a_{21}(+\alpha)](\sigma_\xi^* + \sigma_\xi') + [a_{22}(+\alpha)](\sigma_\eta^* + \sigma_\eta') + [a_{23}(+\alpha)](\sigma_{\xi\eta}^* + \sigma_{\xi\eta}')$$

$$\epsilon_{\xi\eta} = [a_{31}(+\alpha)](\sigma_\xi^* + \sigma_\xi') + [a_{32}(+\alpha)](\sigma_\eta^* + \sigma_\eta') + [a_{33}(+\alpha)](\sigma_{\xi\eta}^* + \sigma_{\xi\eta}')$$

Ply 2

$$\epsilon_\xi = [a_{11}'(-\alpha)](\sigma_\xi^{**} - \sigma_\xi') + [a_{12}'(-\alpha)](\sigma_\eta^{**} - \sigma_\eta') + [a_{13}'(-\alpha)](\sigma_{\xi\eta}^{**} - \sigma_{\xi\eta}')$$

$$\epsilon_\eta = [a_{21}'(-\alpha)](\sigma_\xi^{**} - \sigma_\xi') + [a_{22}'(-\alpha)](\sigma_\eta^{**} - \sigma_\eta') + [a_{23}'(-\alpha)](\sigma_{\xi\eta}^{**} - \sigma_{\xi\eta}')$$

$$\epsilon_{\xi\eta} = [a_{31}'(-\alpha)](\sigma_\xi^{**} - \sigma_\xi') + [a_{32}'(-\alpha)](\sigma_\eta^{**} - \sigma_\eta') + [a_{33}'(-\alpha)](\sigma_{\xi\eta}^{**} - \sigma_{\xi\eta}') \tag{4}$$

Equations linking both plies

$$2\sigma_\xi = \sigma_\xi^* + \sigma_\xi^{**}$$

$$2\sigma_\eta = \sigma_\eta^* + \sigma_\eta^{**}$$

$$2\sigma_{\xi\eta} = \sigma_{\xi\eta}^* + \sigma_{\xi\eta}^{**}$$

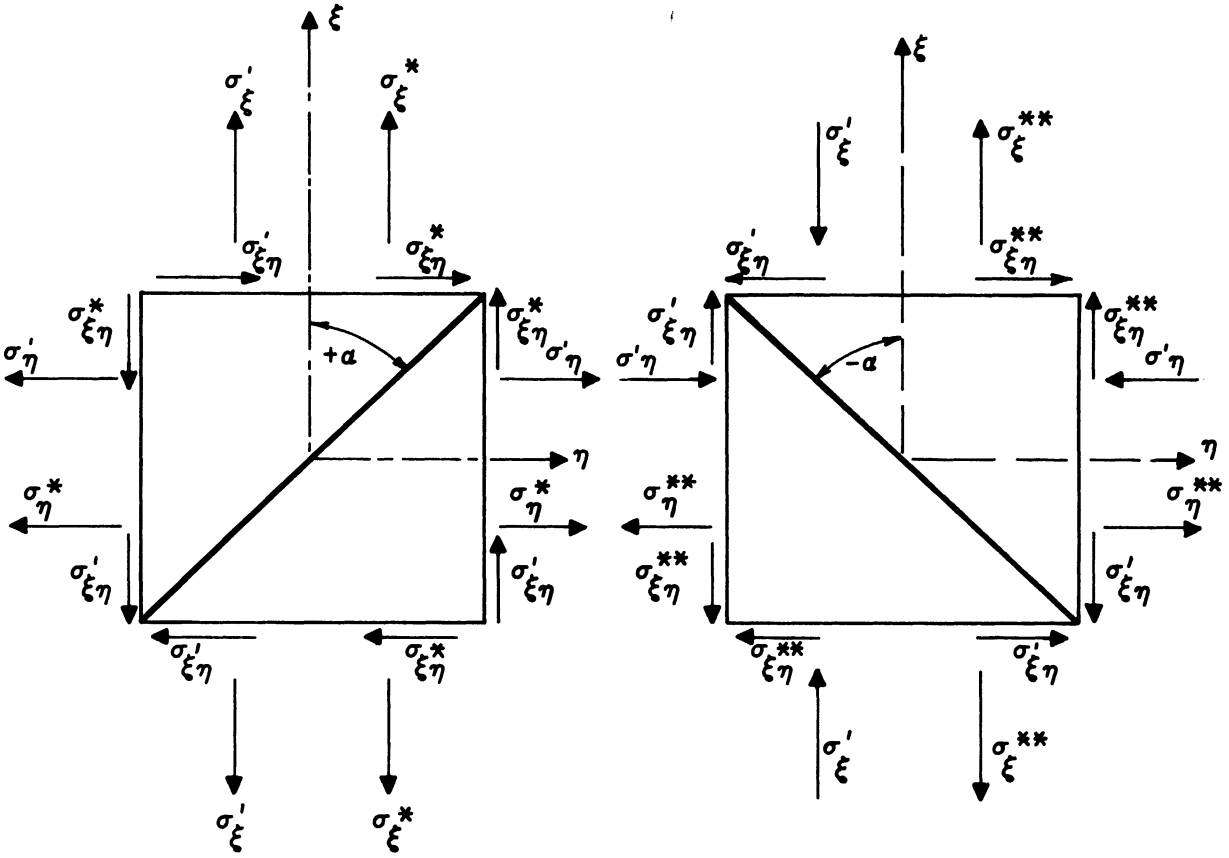

Fig. 8. General plane state of stress on each ply of a two-ply structure.

The first three of Eqs. (4) describe the first ply and utilize constants a_{ij} based on tensile elastic properties of a single sheet. The second three of Eqs. (4) describe the ply whose cords are in compression, and these use a set of a'_{ij} utilizing the compressive elastic constants of a single sheet. The last three of Eqs. (4) are merely a statement that the sum of the stresses carried by the two plies equals the total average stress carried by the composite cord-rubber structure. In writing these equations, the angular argument of the a_{ij} is expressed in parentheses immediately following each term, while primed and unprimed a_{ij} refer to the elastic constants E, F, G being

based on cord compression or cord tension elastic properties respectively.

In these equations the unknowns may be considered to be ϵ_ξ, ϵ_η, $\epsilon_{\xi\eta}$, σ_ξ^*, σ_η^*, $\sigma_{\xi\eta}^*$, σ_ξ^{**}, σ_η^{**}, $\sigma_{\xi\eta}^{**}$, σ_ξ', σ_η', $\sigma_{\xi\eta}'$, assuming that the average external stress σ_ξ, σ_η, and $\sigma_{\xi\eta}$ are given. All the a_{ij} and a_{ij}' terms are known if the elastic properties of individual sheets are known. Thus Eqs. (4) are indeterminate as they stand since there are twelve unknowns with only nine equations. It is clear that three more equations are needed to resolve this indeterminacy.

It was noted in Ref. 1 that the form of these additional equations was not known. It was believed at that time that they depended on a relationship of some kind which would reflect the nature of the elastic bond, probably in the form of some equation linking the interply and applied stresses carried by each ply. Since that time it has been possible to clarify these equations by considering the state of stress at two extreme conditions, one in which the external stresses applied to each ply are completely controlled as independent variables with the interply stresses as dependent variables, the other in which no interply stresses are assumed to exist. A detailed discussion of this point will be given in the subsequent report on interply stresses, but it may be noted here that in either case the elastic characteristics of the structure may be obtained by defining the total stress carried by a ply in the direction of applied load as being the sum of its applied plus interply parts. This removes the necessity for determining the interply portion, and allows the change of variables to be made as follows:

$$\sigma_\xi^+ = \sigma_\xi^* + \sigma_\xi' \qquad \sigma_\xi^{++} = \sigma_\xi^{**} - \sigma_\xi'$$

$$\sigma_\eta^+ = \sigma_\eta^* + \sigma_\eta' \qquad \sigma_\eta^{++} = \sigma_\eta^{**} - \sigma_\eta'$$

$$\sigma_{\xi\eta}^+ = \sigma_{\xi\eta}^* + \sigma_{\xi\eta}' \qquad \sigma_{\xi\eta}^{++} = \sigma_{\xi\eta}^{**} - \sigma_{\xi\eta}' \tag{5}$$

Here a composite or total stress σ^+ or σ^{++} is used to represent the sum and difference of the external and interply stress acting on each ply, respectively. If the new variables σ^+ and σ^{++} are substituted into Eqs. (4), one obtains the following set of equations:

<u>Ply 1</u>

$$\epsilon_\xi = [a_{11}(+\alpha)]\sigma_\xi^+ + [a_{12}(+\alpha)]\sigma_\eta^+ + [a_{13}(+\alpha)]\sigma_{\xi\eta}^+$$

$$\epsilon_\eta = [a_{21}(+\alpha)]\sigma_\xi^+ + [a_{22}(+\alpha)]\sigma_\eta^+ + [a_{23}(+\alpha)]\sigma_{\xi\eta}^+$$

$$\epsilon_{\xi\eta} = [a_{31}(+\alpha)]\sigma_\xi^+ + [a_{32}(+\alpha)]\sigma_\eta^+ + [a_{33}(+\alpha)]\sigma_{\xi\eta}^+$$

<u>Ply 2</u>

$$\epsilon_\xi = [a_{11}'(-\alpha)]\sigma_\xi^{++} + [a_{12}'(-\alpha)]\sigma_\eta^{++} + [a_{13}'(-\alpha)]\sigma_{\xi\eta}^{++}$$

$$\epsilon_\eta = [a_{21}'(-\alpha)]\sigma_\xi^{++} + [a_{22}'(-\alpha)]\sigma_\eta^{++} + [a_{23}'(-\alpha)]\sigma_{\xi\eta}^{++}$$

$$\epsilon_{\xi\eta} = [a_{31}'(-\alpha)]\sigma_\xi^{++} + [a_{32}'(-\alpha)]\sigma_\eta^{++} + [a_{33}'(-\alpha)]\sigma_{\xi\eta}^{++} \tag{6}$$

<u>Equations linking both plies</u>

$$2\sigma_\xi = \sigma_\xi^+ + \sigma_\xi^{++} = \sigma_\xi^* + \sigma_\xi^{**}$$

$$2\sigma_\eta = \sigma_\eta^+ + \sigma_\eta^{++} = \sigma_\eta^* + \sigma_\eta^{**}$$

$$2\sigma_{\xi\eta} = \sigma_{\xi\eta}^+ + \sigma_{\xi\eta}^{++} = \sigma_{\xi\eta}^* + \sigma_{\xi\eta}^{**}$$

In Eqs. (6) the σ^{+} and σ^{++} may be treated as unknowns. In this case there are nine equations and nine unknowns for which a complete solution may be made. This solution will be exact and will reflect the effects of all possible loading mechanisms. Elastic stiffnesses may be obtained from this set of nine equations, but it will not in general be possible to separate the fractions of externally applied stress carried by a given ply from the stress generated by interply forces carried by the same ply, all in a given direction. The implications of this will be discussed in some detail in an additional report concerning interply stresses in Type 2 laminates.

The solution of Eqs. (6) by hand would be a long and tedious process for cases of general stress application. For that reason a digital computer program was written for the solution of these nine simultaneous equations in terms of the various ratios of stress to strain. Most of the calculations presented here were performed digitally by this program which was found quite convenient for that purpose.

It was next necessary to design experiments in which the elastic characteristics of a Type 2 structure could be determined experimentally. These data could then be compared with predictions from the digital solution to Eqs. (6). Accordingly, the same experimental apparatus which was used for obtaining the shear modulus of Type 1 laminates was used here to obtain the extension modulus and cross modulus of Type 2 laminates. This was done by using the tubular specimen described in Ref. 1 in this same combined tension-torsion-internal pressure loading device. Now, however, the loads were applied in a different order. Each specimen was first subjected to a twist

or torque which caused one set of cords to go into tension while another set of cords went into compression. Next, axial loads were applied by means of the hydraulic cylinder. Measurement of the corresponding extension and contraction along with simultaneous measurement of the axial loads allowed one to calculate the elastic stiffnesses of the structure. The mechanical equipment and recording apparatus was identical to that described earlier in this report. In Fig. 9, the ratio of applied axial stress to resulting axial strain is plotted as measured from these experiments. The original data are corrected for angular change as previously discussed. It is also corrected for possible changes in the diameter of the tubes in question. Also plotted in Fig. 9 is the ratio axial stress to resulting axial strain as calculated from the machine solution to the nine simultaneous Eqs. (6). Again, it is seen that correlation between experiment and theory is relatively good. In Fig. 10 a similar comparison is shown between the radial contraction of the tubes compared with the imposed axial stresses. This quantity was previously denoted as F when dealing with orthotropic structures. It is again seen that measured data correlates well with the calculations from Eqs. (6).

In Fig. 11 both experimental data and the results of calculations made from Eqs. (6) are presented for the ratio of shearing stress to shearing strain as a function of cord angle for a Type 2 structure. Comparing these results with Fig. 7, the comparable presentation for the Type 1 structure, it may be seen that the stiffnesses presented here are fully an order of magnitude less than those discussed in Fig. 7. In Fig. 11, the upper curve

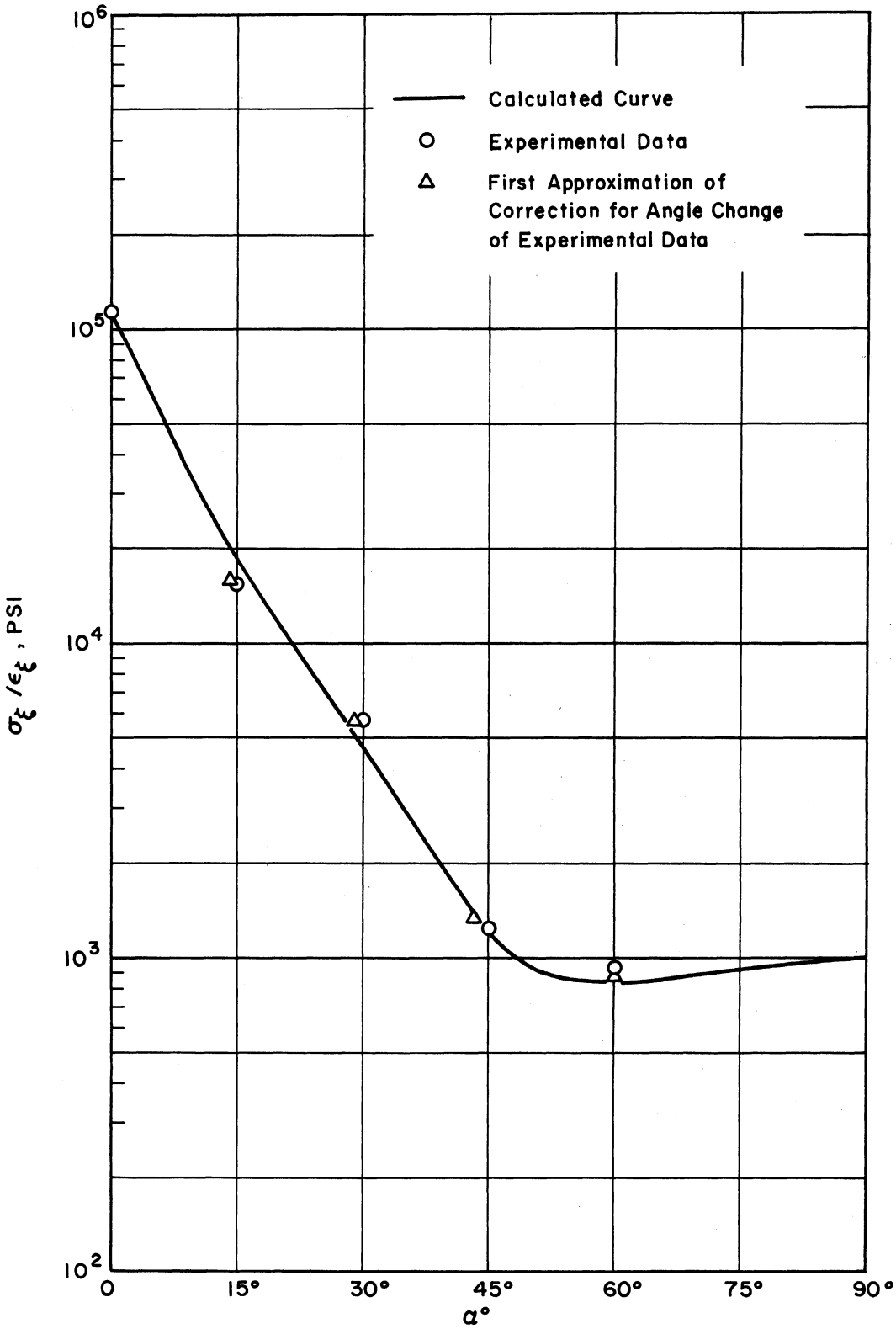

Fig. 9. Ratio σ_ξ/ϵ_ξ vs. cord half angle α, as predicted from Eq. (5) of this report with $\sigma_\eta = \sigma_{\xi\eta} = 0$, along with experimental values of this ratio, for a Type 2 structure.

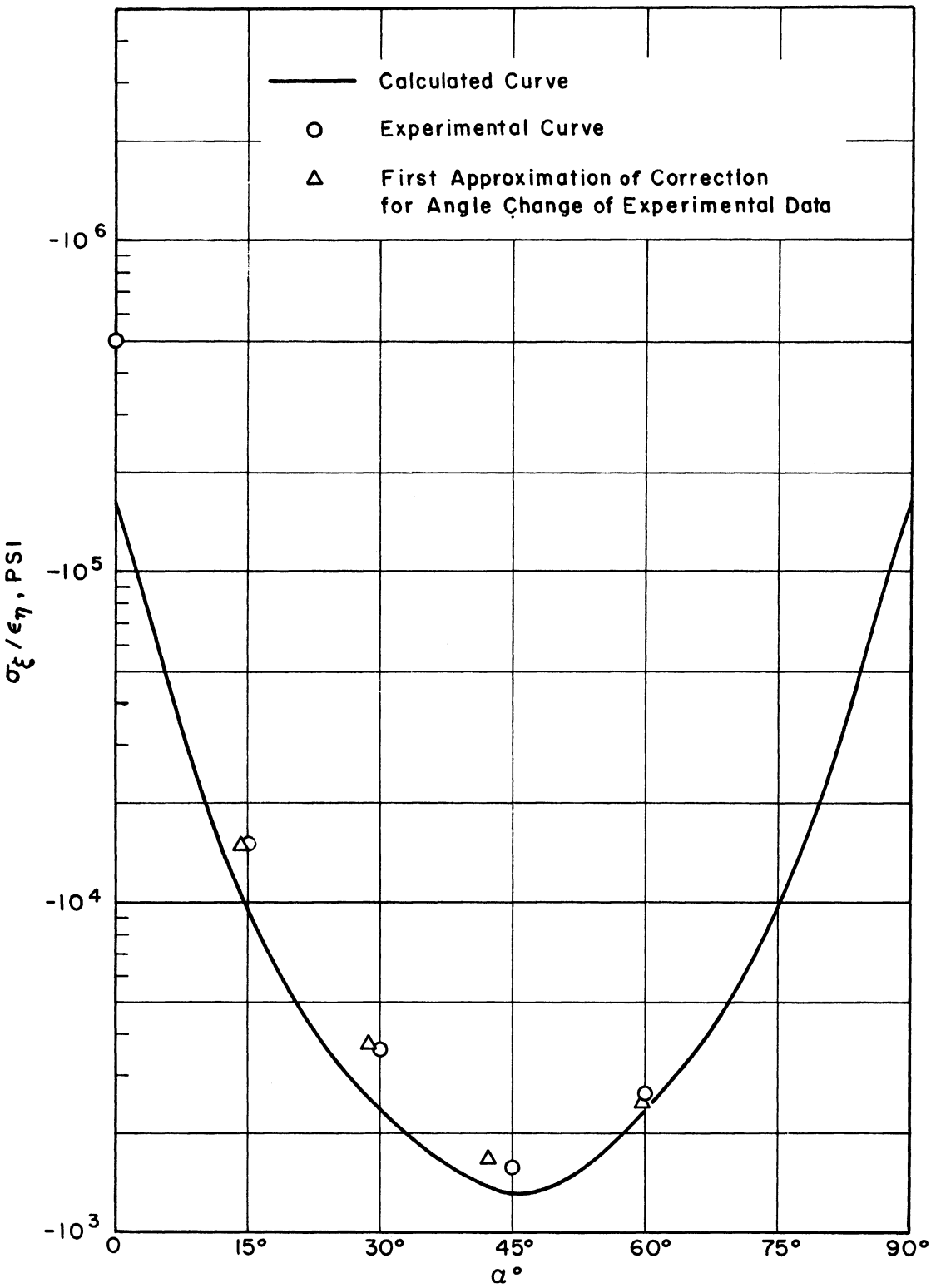

Fig. 10. Ratio σ_ξ/ϵ_η vs. cord half angle α, as predicted from Eq. (5) of this report with $\sigma_\eta = \sigma_{\xi\eta} = 0$, along with experimental values of this ratio, for a Type 2 structure.

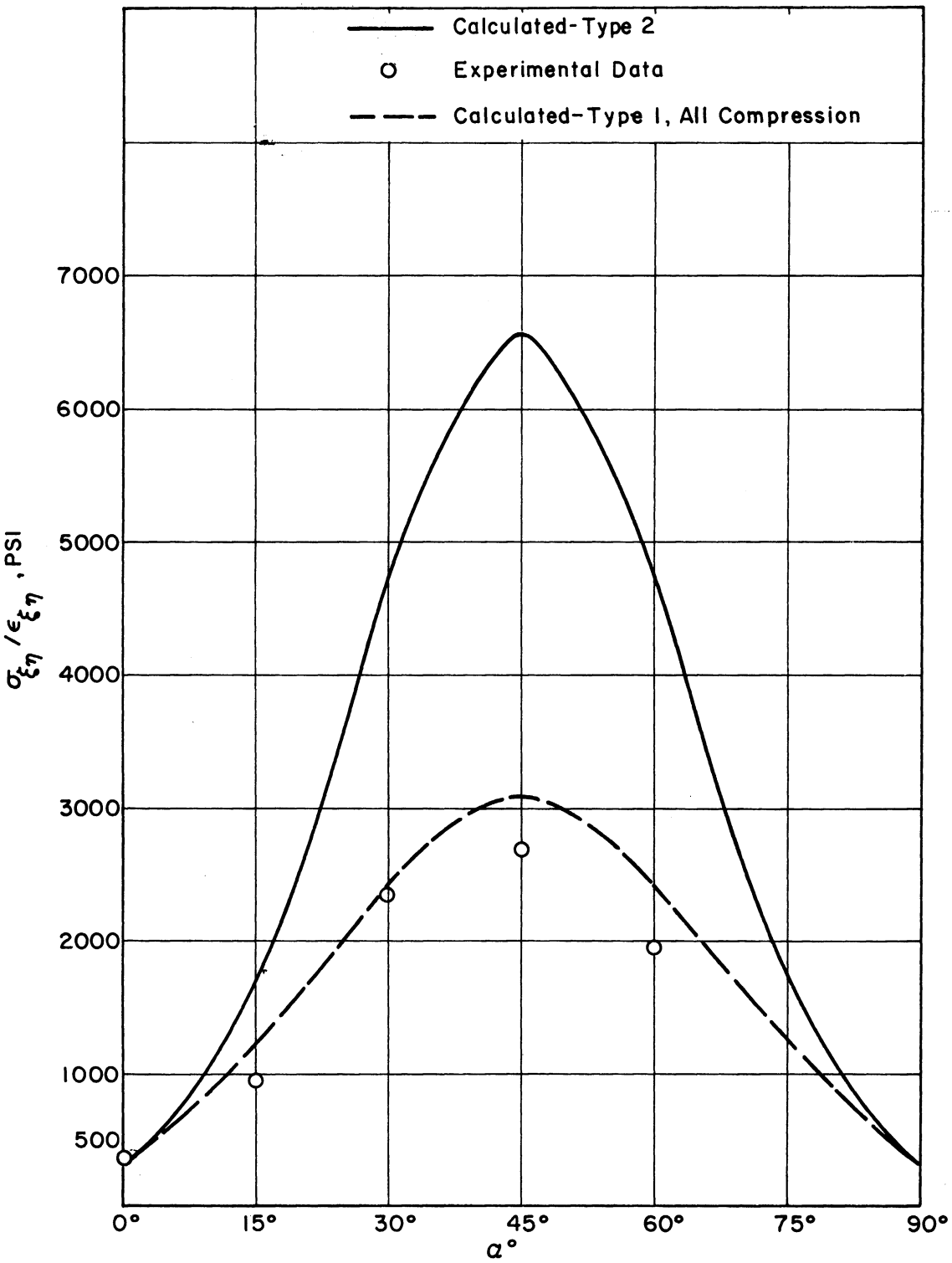

Fig. 11. Ratio $\sigma_{\xi\eta}/\epsilon_{\xi\eta}$ vs. cord half angle α, as predicted from Eq. (5) of this report with $\sigma_\eta = \sigma_\xi = 0$, along with experimental values for this ratio, for a Type 2 structure.

represents the values of the ratio shear stress to shear strain as predicted from the solutions to Eqs. (6). This postulates the existence of well-developed tensile and well-developed compressive strains in cords in alternate plies.

The experimental data which are presented in Fig. 11 were obtained from the cylindrical specimens previously described. For this series of tests, these specimens were twisted in a standard torsion machine without any additional axial load being applied. Due to the thin-walled nature of these specimens, only very low torsional moments could be applied before buckling took place. For that reason it was not possible to stress these specimens sufficiently to cause the well-developed tensile portion of the structure to manifest itself, that is to say, it was not possible to load the tension-carrying cords heavily enough to cause their stiffness to be represented well by the tensile modulus of the cords. For this reason, it was not possible to develop as great a stiffness with these specimens as is predicted by Eqs. (6). This is felt to be a fault of the design of the specimens and not of the analytical development leading up to Eq. (6).

It might be argued with some justification that if it was not possible to load the tension-carrying cords into a state where their stiffness was represented by the well-developed tensile modulus, then one might suspect that the over-all stiffness in shear of this structure might be approximated much better by an equation such as Eq. (2), but now using the compressive elastic stiffnesses of all materials. This would assume implicitly that the strains in a tube under low values of torsion were small enough so that

essentially compressive moduli prevailed throughout the tube. Using this assumption, it is possible to calculate once more the ratio of shearing stress to shearing strain and these values are also shown in Fig. 11. It may be seen that the experimental data agrees much more closely with the predicted values from Eq. (2) than with the predicted values from Eqs. (6).

It is believed that the use of specimens designed particularly for this type of test would allow much larger values of torque to be applied and would result in better agreement with Eq. (6). However, it is also believed that the explanation for the good agreement of experimental data with results as predicted by Eq. (2), using compressive sheet elastic properties, is in itself instructive since it provides an example of the fact that these structures are extremely dependent upon the state of cord load for their stiffness. Furthermore, it also illustrates the fact that at many cord angles it is rather difficult to load the cords heavily and that in these conditions the stiffnesses of the structure tend toward those stiffnesses predicted upon the basis of compressive elastic characteristics. It is believed that this is a generalization of the phenomena known as "soft-stretch" often encountered in the tensile testing of textile cords.

Again comparing Figs. 7 and 11, it should be mentioned that the results of Fig. 7 were obtained by the application of internal pressure and tensile loads to these tubular specimens. These loads were sufficient to strain the cords enough so that an appreciable change in their stiffness occurred. This stiffness change caused, in turn, a stiffness increase in the over-all tube resulting in the much higher stiffnesses reported in Fig. 7 as compared

to those reported in Fig. 11. Thus, the differences between the results of Fig. 7 and Fig. 11 are simply those differences caused by the application of tensile loads to the cords. For that reason, they throw light on the workings of this phenomena of modulus change near the origin and are wholly consistent with all theoretical work done so far and with our previously stated ideas concerning how this change occurred. It is most evident here in the measurement of shear modulus or its anisotropic equivalent, since in these quantities cord stiffness plays a dominant role in the over-all stiffness of the body over the whole possible range of cord angles. In the measurement of extensional modulus, cord stiffness is not such a glaringly dominant factor over the entire range of cord angles.

APPENDIX

SAMPLE CALCULATIONS FOR CORRECTION OF CORD ANGLE DUE TO STRAIN

The example presented here is designed to illustrate an approximate method for correcting experimental data taken on cord-rubber laminates. As mentioned in the body of the report, any finite amount of strain in a specimen results in some angular change of the cords with respect to one another. In many cases this effect is significant since the change of stiffness with angle may be quite large. For that reason, a first approximation to this correction may be based on an approximate value of Poisson's ratio obtained from theoretical considerations. Additional approximations could be made based on the results of the first approximation, but in general they are not warranted. The calculations for a representative 30° specimen are presented below:

Example: 30° Specimen

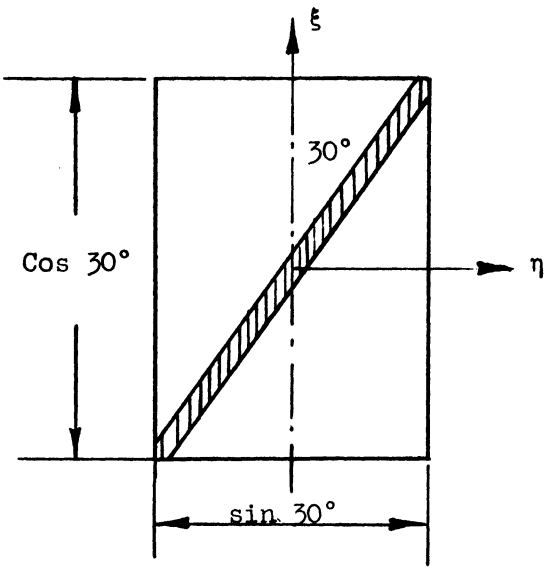

Before Deformation

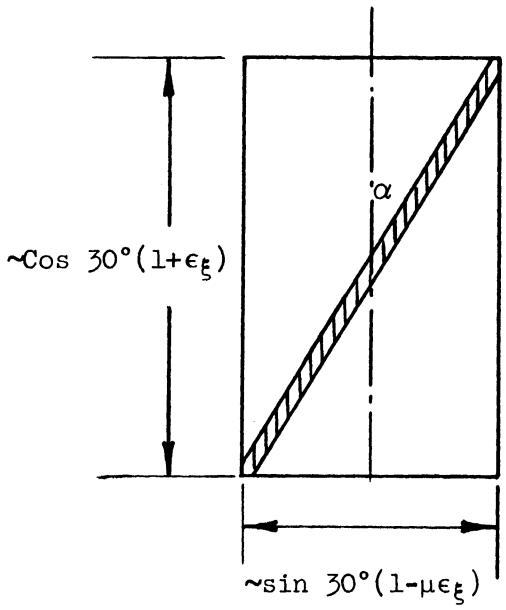

After Deformation

For E_ξ

μ = 2.8 - theoretically from Fig. 18, Ref. 1.

$\epsilon_\xi \approx$ .025 - from experimental data.

$$\tan \alpha \approx \frac{\sin 30°(1-\mu\epsilon_\xi)}{\cos 30°(1+\epsilon_\xi)} = \frac{.500[1-2.8(.030)]}{.866[1+.030]} = 0.5134$$

$\alpha \approx 27° \; 11'$ This is the corrected cord angle to the first approximation.

V. ACKNOWLEDGMENT

The authors of this report wish to acknowledge the assistance of Dr. Bertram Herzog, who constructed and wrote the digital computer program which was used to obtain the solutions to Eqs. (6) in this report. They would also like to acknowledge the assistance of Mr. D. H. Robbins who aided in obtaining experimental data presented here.

VI. REFERENCE

1. S. K. Clark, The Plane Elastic Characteristics of Cord-Rubber Laminates, The University of Michigan Research Institute, Tech. Report 02957-3-T, Ann Arbor, Michigan.

VII. DISTRIBUTION LIST

	No. of Copies
The General Tire and Rubber Company Arkron, Ohio	6
The Firestone Tire and Rubber Company Akron, Ohio	6
B. F. Goodrich Tire Company Akron, Ohio	6
Goodyear Tire and Rubber Company Akron, Ohio	6
United States Rubber Company Detroit, Michigan	6
S. S. Attwood	1
R. A. Dodge	1
The University of Michigan Office of Research Administration File	1
S. K. Clark	1
Project File	10

UNIVERSITY OF MICHIGAN
3 9015 02539 7012